An Improved Calibration Technique for Coupled Single-Row Telemeter and CCD Camera

Romain Dupont, Renaud Keriven
C.E.R.T.I.S.[*]
Ecole Nationale des Ponts et Chaussees
6-8 Avenue Blaise Pascal
Champs-Sur-Marne, 77455, France
Email: {dupont,keriven}@certis.enpc.fr

Philippe Fuchs
E.N.S.M.P.
60, Bd Saint-Michel
Paris, 75272, France
Email: fuchs@ensmp.fr

Abstract

Toward a successful 3D and textural reconstruction of urban scenes, the use of both single-row based telemetric and photographic data in a same framework has proved to be a powerful technique. A necessary condition to obtain good results is to accurately calibrate the telemetric and photographic sensors together. We present a study of this calibration process and propose an improved extrinsic calibration technique. It is based on an existing technique which consists in scanning a planar pattern in several poses, giving a set of relative position and orientation constraints. The innovation is the use of a more appropriate laser beam distance between telemetric points and the planar target. Moreover, we use robust methods to manage outliers at several steps of the algorithm. Improved results on both theoretical and experimental data are given.

1 Introduction

For urban planning, the heritage safeguard or the creation of virtual environments (3D cartography, cinema, video games), there is a growing interest for automatic digitization of urban environments. One way to build accurate 3D textured urban models is to merge two kinds of data : telemetric data acquired with a single-row telemeter and photographic data obtained via a CCD camera. These two sensors are rigidly fixed on a moving car as in [9], [3], [1]. While the car is moving through the city, the telemeter acquires 2D profiles which are put in the same reference, giving a cloud of 3D points (figure 1 shows an example of such a point cloud). In same time, the CCD camera acquires a sequence of images which are mainly used to obtain textures and structure information via stereovision.

This method of digitization has proved to be an efficient way to quickly obtain satisfactory 3D textured urban models. To use both telemetric and photographic data in a same framework, the geometrical transformation between the Telemeter and the Camera references must be known accurately. If such calibration techniques exist for system based on lighting telemeters (in such case, the laser beam is visible) [5], [6], there are few results for telemeters with invisible beam. One major work is the one published by Pless & Zhang in [7]. They propose an extrinsic calibration process : they scan a planar pattern (a chessboard) in several poses with the telemeter and the camera, giving a set of relative position and orientation constraints. An optimization via a gradient descent method is done to get the extrinsic parameters between the sensors.

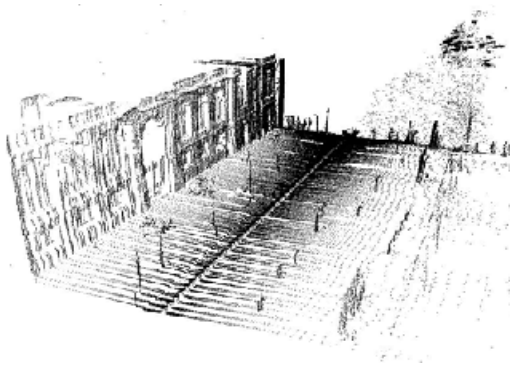

Figure 1. Point cloud of an urban environment

This paper studies this telemeter / camera calibration process. Several improvements of this technique are proposed : in [7], the residual to be minimized is the orthogonal distance between the telemetric points and the target plane. Yet the variances of estimation errors are not equal for each angle of sight, inducing a bias. We introduce a more ap-

propriate distance, which is still the distance between the telemetric points and the target plane *but along the ray of the laser beam* and hence not orthogonally. Furthermore, we introduce robust methods to manage outliers at several steps of the algorithm.

The outline of this paper is as follows: Section 2 presents the acquisition system and its characteristics. Section 3 presents the laser/camera calibration process. The introduction of the new distance will be described. Section 3.4 presents a more robust method for the relative orientation estimation. Lastly, results on both synthetic and experimental data are presented in Section 4.

2 Acquisition system overview

Our system is composed of a telemeter and a CCD camera hard-linked through a support. The 'optical center' of the telemeter is put close to the camera one, reducing the occlusions due to a shifted point of view (see figure 2 for an example of such a support).

Figure 2. Telemeter / CCD Camera support (there are two cameras, but here, only the left one is used).

2.1 Telemeter characteristics

Our telemeter is a single-row one and so sweeps a plane in space. It gives for each angle of sight the distance to the first obstacle. Its laser beam is invisible (class 1 IR laser) and its distance estimation accuracy is about 5 cm whatever the distance to the first obstacle is. Last but not least, the laser beam is not a perfect thin cylinder but its form is slightly conical: at high distance, we can encounter erroneous distances, especially near the edges. This last phenomena must be taken into account while observing the results.

2.2 Camera calibration

The calibration target (ie. the chessboard) is placed in front of the camera. The camera calibration process is done via Matlab with the *Matlab Calibration ToolKit* which uses standard calibration methods ([2], [8]). The reprojection accuracy is sub-pixel (less than 0.3 pixel). Extrinsic parameters are estimated with an error less than 0.25 °for rotation parameters, and less than 1 cm for translation parameters. These values are computed during the calibration process [1]. Actually, the accuracy depends on other parameters, such as the accuracy of the measures of the dimensions of the target (or the size of a square of the chessboard). These errors have been estimated empirically as about 3% of the distance. This must be taken into consideration because the calibration process evolves in a metric reference.

2.3 Why not calibrating manually ?

Such a support allows several relative positions and orientations between the telemeter and the camera. One can approximate them manually and rigorously (which is done in general) but it will be inaccurate:

- an error of about one degree in the estimation of the orientation of telemeter bring important error at high distances (for example, 1 degree covers 35 cm at 20 meters from the telemeter). Moreover, it is difficult to estimate manually the angles around Y-axis and Z-axis (drawn in figure 4).
- and the position of the optical center of the telemeter is generally unknown, and not necessarily at the center of the rotating head.

3 Calibration technique

We want to estimate R (rotation matrix) and T (translation vector) such that:

$$P_L = RP_C + T$$

with $P_L = (X_L, Y_L, Z_L)^T$ the coordinates of laser points in the Telemeter reference $\mathcal{R}_L$ and $P_C = (X_C, Y_C, Z_C)^T$ in the Camera reference $\mathcal{R}_C$ [2]. A Euclidean transformation has been chosen. Indeed, the scale of $\mathcal{R}_C$ and $\mathcal{R}_L$ are the same (in millimeters) and an affine or projective transformation are useless.

The general principle is to present a planar target with a chessboard (fig. 3) in front of the laser/camera support. The telemeter scans the target, giving a 2D profile (segment in space) while the camera is capturing an image of the chessboard. From this image, we extrinsically calibrate

[1] These errors are three time the standard deviation of estimation errors (details are available on the web site: `http://www.vision.caltech.edu/bouguetj/calib_doc/`)

[2] Note: Telemetric point coordinates P_L are always in the form $(0, Y, Z)^T$ in $\mathcal{R}_L$, because they belong to the plane X=0

the camera. Extrinsic parameters are then used to estimate the target plane parameters (N,d) in the Camera reference such as $N \cdot x = d$ with N normalized.

Figure 3. Planar target with a chessboard

These telemetric points necessarily belong to the target plane, inducing constraints which are used to compute the relative position and orientation between $\mathcal{R}_C$ and $\mathcal{R}_L$. However, these constraints would be insufficient to estimate correctly R et T if we let the target static. Additional constraints will be obtained by moving the target in several poses (rotations around the vertical and horizontal axis).

3.1 Formalization

The laser reference $\mathcal{R}_L$ is orthogonal direct, like the Camera reference $\mathcal{R}_C$. Figure 4 shows the axis directions.

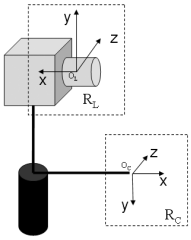

Figure 4. Telemeter reference $\mathcal{R}_L$ and Camera reference $\mathcal{R}_C$

When the telemeter sweeps the target, telemeter points P_L belong to the chessboard and so verify:

$$\begin{aligned} N \cdot P_C - d &= 0 \\ \text{i.e.} \quad N \cdot \left[R^{-1}(P_L - T)\right] - d &= 0 \end{aligned}$$

with d, the distance between the target plane and the camera, N the plane normal in $\mathcal{R}_C$ (N normalized). The target is moved in $\mathcal{N}$ poses and we estimate R and T by minimizing

$$\mathcal{E} = \sum_{i}^{\mathcal{N}} \sum_{j} D_{ij}^2(R,T)$$

with D_{ij}, the distance from the j-th point P_{C_j} of the i-th pose of the target. Rather than choosing the algebraic (ie. orthogonal) distance $N \cdot P_C - d$, which is inadequate here (the variances of the distance errors are not equal for each angle of sight), we use the distance D *along the laser beam* $\vec{r}$ (of center s) between the point $P_C = R^{-1}(P_L - T)$ and the target plane:

$$D_{ij} = \left\| P_C - (s + \vec{r} * T) \right\|$$

with

$$\begin{aligned} T &= \frac{(-d + N \cdot s)}{N \cdot \vec{r}} \\ \vec{r} &= (P_C - s) \\ s &= -R * T \end{aligned}$$

Intuitively, T is the time of collision between the target plane and the ray $\vec{r}$ passing through the center s . The figure 5 shows theses distances.

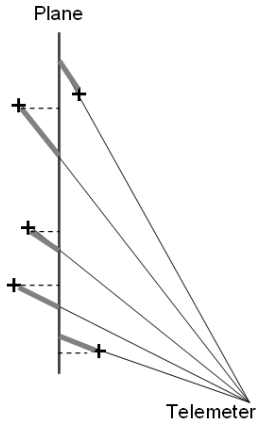

Figure 5. The bold lines represent the residual distances along the laser beam. The dotted lines represent the orthogonal distances and the crosses represent telemetric points.

3.2 Rotation representation

The rotation matrix R is replaced by a couple (V,α), where the vector V represents the direction of the principal rotation axis and α, the angle around this axis. Posing

$\alpha = \|V\|$, this representation (also called *Rodriguez Representation*) takes three parameters and avoids problems met with the 'Euler Representation' which is not unique and not continuous everywhere and thus inadequate for optimization process.

3.3 Calibration process

We present the target in front of the camera/laser support and, for each pose of the target, we extract several n 2D telemetric profiles and one image of the target. Multiplying the profiles reduces the error of the distance estimation by computing, for each angle of sight, a robust mean of the n given distances x_i. We proceed as follows: we compute the robust residual σ, also called *median absolute deviation* (MAD) through

$$\sigma = 1.48 \underset{i}{median} |x_i - \underset{j}{median} |x_j| |.$$

We pose $r_i = x_i - median_j |x_j|$ the residual for each point x_i. Good results and robustness against outliers have been obtained by removing points with $|r_i| > 4.7\sigma$ as recommended in [4]. Then, we recalculate the residual without the outliers and so on until stabilization. Thus, the accuracy increases: the estimation error evolves from 5 cm to less than 1 cm. Then, these 3D points are segmented via a simple algorithm which separates telemetric points belonging to the target (these points are in front of the telemeter) from the others (see figure 6). The function to be minimized is not linear, thus the minimization of $\mathcal{E}$ is done with the Levenberg-Marquardt optimization algorithm. Results are presented in section 4.

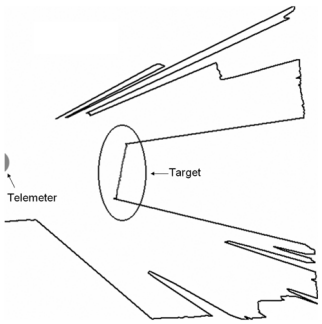

Figure 6. Segmentation of the horizontal telemetric 2D profile (view from above): on the left, the origin of the telemeter and in the middle, the points of the target automatically extracted.

Note that the single-row telemeter accuracy is generally of about 5 cm, whatever the distance of the first obstacle. So, for high distances, the relative accuracy of the telemeter increases. Hence, the planar target must be as far away as possible from the telemeter and have a large size such that the camera sees it with good resolution. In our configuration, its size is about 100*100 cm^2.

3.4 Robust estimation of the relative orientation

If objects to be digitized are far away from the acquisition system, the accuracy of the relative position between the two sensors is less important but the orientation becomes critical. The method proposed above gives good results but it is not robust against erroneous telemetric points (outliers) and somes poses of the target may be inaccurate due to their important angle with respect to the camera.

We add a two-steps post-processing algorithm: the first step removes telemetric points whose residuals are more than 4.7 robust deviation (MAD) away from the median of all residuals $D_{ij}^2(R,T)$. After removing them, we re-estimate R and T without the outliers, and so on until no new outlier is detected (about 3 iterations are generally needed). Moreover, in the second step, we apply the same principle to remove poses which have a too much high global residual. Results will be discussed in 4.2.

4 Results

These approaches are compared here, both on synthetic and real data.

4.1 Synthetic data

Toward a ground-truth comparison, we generate synthetic data via the following method: we fix T and R and we determine n plane equations in $\mathcal{R}_C$, corresponding to n target poses. These equations are those computed during the experiments, in order to be close to the experimental framework. These equations are then expressed in $\mathcal{R}_L$, we simulate the emission of laser beams (the sweeping range of the telemeter is empirically determined) and we compute their intersections with the target plane. In cylindrical coordinates, distances are noised according to the measured telemeter characteristics (in our configuration, it is an IBEO telemeter: the noise is Gaussian with a standard deviation of 5 cm).

Results are summarized in tables 1 and 2. The table 1 gives the number of iterations needed to converge to the same accuracy and in the second column, the residual error of the estimation of the relative position between the telemeter and the camera (expressed in millimeters). The table 2 gives the residual of the relative orientation between the two sensors. The errors in rotation depend on several

Method	nb of iter.	transl. error
Orthogonal distance (Pless and Zhang [7])	1500	5 mm
Our method	300	1.5 mm

Table 1. Synthetic data: relative position estimation

parameters, mainly the axis of rotation and the initial parameters used for the optimization process. These errors are grouped into an interval, explaining the presence of the symbol $\pm$ into the table. Gaussian noise has been added with two standard deviation: 10 and 50 mm.

Method	rotation error noise 10 mm	rotation error noise 50 mm
Orthogonal dist. (Pless & Zhang [7])	0.03 ± 0.03 °	0.30 ± 0.06 °
Our method	0.015 ± 0.015 °	0.05 ± 0.03 °

Table 2. Synthetic data: relative orientation estimation

The use of the distance along the ray increases the overall accuracy for both translation and orientation estimations. Particularly, rotation errors are divided by two. Moreover, we notice an improved robustness against local minima throughout our experiments. Several experiments have shown that even when we set a coarse initialization (up to 30 ° of error from the exact orientation), the optimization process recovers the global minimum.

4.2 Experimental results

There is no ground-truth data to compare numerically the accuracy of the calibration process. We use the virtual projection of the telemetric points into images as a comparative criterion.

Figures 7 and 8 show these points projected using parameters obtained via calibration on several objects and environments. We can see that the telemetric points are correctly projected. Note that the optical center of the telemeter does not coincide with the camera one, so some objects seen by the telemeter are not seen by the camera. Hence, in figures 7 and 8, we can observe the presence of some projected points which looks erroneous but this is just due to occlusions.

Figures 9, 10 and 11 show telemetric points projected on a facade. Telemetric point are more accurately projected

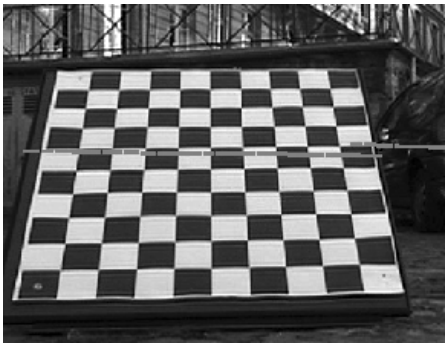

Figure 7. Projection of telemetric points with our distance

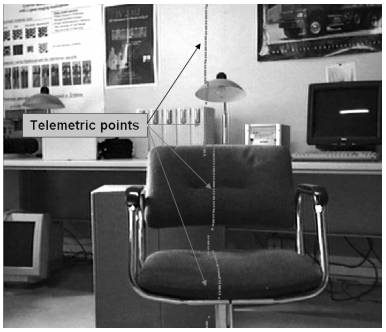

Figure 8. Projection of telemetric points with our distance

with our distance. As mentioned in the subsection 2.1, the presence of points above the facade are due to the telemeter characteristics and not to the calibration.

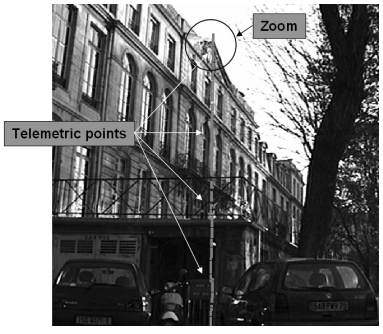

Figure 9. Projection of telemetric points on a facade with our distance

In addition, in most cases, no pose has been removed

throughout the process: the plane orientation of each target has always been well estimated. Furthermore, a small amount of erroneous telemetric points has been removed during the robust step of the calibration. This is due to the great quantity of available telemetric points and to the robust mean computed just after acquiring several 2D telemetric profiles (as detailed in the subsection 3.3).

Figure 10. Zoom of the projection of telemetric points on a facade with orthogonal distance.

5 Conclusion

We have made an extended study of the calibration process and we propose an improved technique which uses both a more appropriate distance and robust statistics. It has been extensively tested on both synthetic and real data. For applications requiring to build accurate 3D models, it gives satisfactory results in regards to the characteristics of the telemeter and the camera. Telemetric points are well virtually projected on corresponding images.

Figure 11. Zoom of the projection of telemetric points on a facade with our distance.

References

[1] I. Abuhadrous, S. Ammoun, and al. Digitizing and 3d modeling of urban environments and roads using vehicle-borne laser scanner system. *IEEE/RSJ International Conference on Intelligent Robots and Systems, Sendai, Japan*, Sept 2004.

[2] Olivier Faugeras. *Three-dimensional computer vision: a geometric viewpoint*. MIT Press, 1993.

[3] Christian Fruh and Avideh Zakhor. An automated method for large-scale, ground-based city model acquisition. *Int. J. Comput. Vision*, 60(1):5–24, 2004.

[4] P.W. Holland and R.E. Welsch. Robust regression using iteratively reweighted least squares. *Comm. Statistics Theory and Methods*, vol. A6:813–827, 1977.

[5] Olli Jokinen. Self-calibration of a light striping system by matching multiple 3-d profile maps. In *2nd International Conference on 3D Digital Imaging and Modeling (3DIM '99), Ottawa, Canada*, pages 180–190, 1999.

[6] Alan M. McIvor. Calibration of a laser stripe profiler. In *2nd International Conference on 3D Digital Imaging and Modeling (3DIM '99), Ottawa, Canada*, pages 92–98, 1999.

[7] Robert Pless and Qilong Zhang. Extrinsic calibration of a camera and laser range finder. In *IEEE International Conference on Intelligent Robots and Systems (IROS)*, 2004.

[8] Zhengyou Zhang. Flexible camera calibration by viewing a plane from unknown orientations. In *7th IEEE International Conference on Computer Vision*, pages 666–673, 1999.

[9] Huijing Zhao and Ryosuke Shibasaki. Reconstructing textured cad model of urban environment using vehicle-borne laser range scanners and line cameras. In *Machine Vision and Applications*, volume 7, pages 35–41, 2003.